DOI: https://doi.org/10.57233/ijsgs.v11i3.915 ISSNp: 2488-9229; ISSNe: 3027-1118

IJSGS FUGUSAU VOL. 11(3) WEBSITE: https://fugus-ijsgs.com.ng

INTERNATIONAL JOURNAL OF SCIENCE FOR GLOBAL SUSTAINABILITY
(A PUBLICATION OF FACULTY OF SCIENCE, FEDERAL UNIVERSITY GUSAU, NIGERIA)

Flood Risk Mapping in the River-Rima Basin, Kebbi State, Nigeria: A Geographic Information System-Based Approach

M. Aliyu* , L. Ahmad, H. A. Adigun, R. M. Jega, Z. M. Bako

Department of Agricultural and Bio-Environmental Engineering,Technology,Waziri Umaru Federal Polytechnic, Birnin Kebbi, Nigeria.

***Corresponding Author's Email:** muzzammilaliyu@wufpbk.edu.ng

Received on: August, 2025 **Revised and Accepted on:** September, 2025 **Published on:** October, 2025

ABSTRACT

Floods are a growing menace to human life, as well as to infrastructure and agricultural yields in emerging river floodplain regions. The River Rima floodplain is well known in Birnin Kebbi for its agricultural production, especially rice production, which is essential to local livelihood and food security. This study employs an integrated GIS and Analytic Hierarchy Process (AHP) approach to evaluate flood risk zones within the River Rima basin, Nigeria. Six geomorphological and hydrological factors (elevation, slope, drainage density, rainfall, soil type, and land use) were weighted through pairwise comparisons to generate hazard and vulnerability indices. The Flood Hazard Index was accomplished. Settlement distribution was taken as a susceptibility criterion to create the Flood Vulnerability Index. By linking these maps with indices, a flood risk map was generated, which shows that the study area is divided into high (25.29%), moderate (29.64%), and low (45.07%) flood risk classes, indicating that more than half of the floodplain is at risk of floods. The research identifies six main flood hazard predictors: elevation (38.1%), drainage density (19.6%), slope (17.8%), mean annual rainfall (12.2%), soil type (6.4%), and land use (6.0%). This means that elevation and drainage density, which are geomorphological factors, play a major role in causing floods in the area. Urban expansion poses a great threat to settlements like Ambursa, Birnin Kebbi, and Dagere, whereas settlements like Makerah, Anguwar Kayi, and Maurida are located in the floodplain and are therefore very prone to the effects. Farmland and built-up land are the most at-risk elements, with 64.7% of farmland and 70.2% of built-up areas classified as highly or moderately vulnerable. Based on these findings, the study recommends incorporating land-use zoning, community-based flood preparedness, and relocating critical infrastructure. The implementation of long-term planning strategies demands both climate change projections and machine learning technologies for future flood modelling.

Keywords: Flood Risk, GIS, AHP, Vulnerability, Mapping,

1.0 INTRODUCTION

Floods are one of the most dangerous natural disasters, and they often happen without much warning (FEMA, 2020). Flooding is one of the worst natural disasters in the world. It has a domino effect on people's safety, infrastructure, and the productivity of farms (UNDRR, 2022). In Nigeria, riverine floods cause 60% of the country's annual disaster losses, especially in low-lying areas like the River Rima (NIHSA, 2023). Climate change makes rainfall more variable (IPCC, 2021), and human activities like encroaching on floodplains make the risks even worse (Ajibade et al., 2013).

FEMA (2020) reports that in Nigeria, flooding predominantly occurs during the rainy season, especially within floodplains adjacent to major rivers and their tributaries, consistent with NIMET's meteorological projections. For example, NIMET predicted in 2020 that floods caused by high rainfall could cause delays in development, impede traffic, and damage infrastructure like roads, tunnels, and bridges. Low-lying locations close to rivers are typically affected by riverine floods (Risi, 2020). The Agency on Hydrological Services in Nigeria, (NIHSA, 2019) suggested that 12 LGAs in Kebbi State, such as those of Birnin Kebbi, Kalgo, and Shanga, would be susceptible to seasonal flooding. is mostly attributed to the hydrologic activity of the rivers Sokoto, Gagare, Bunsuru, Maradi and Zamfara, coupled with the controlled releases of the Bakolori and Goronyo dams that raise the volumes of flow downstream along other rivers, especially the river Rima during the rainy season. The River Rima floodplain, located in Birnin Kebbi, Nigeria, experiences frequent and severe flood events every year due to its hydrological and topographical features. The rising floods in this region, in terms of their frequency and high intensity, require newer and more sophisticated procedures. The given application of GIS bilateral consensus decision-making demonstrates a more detailed and spatially sophisticated process of hazard/risk management in comparison with the approach of earlier flood risk evaluation, most often based upon empirical models and historical data about floods (Samela et al., 2018). Moreover, the products of the geospatial technology, which include GIS and remote sensing, have been functional and of a big benefit in the establishing of disaster management schemes. Most areas across the globe have been mapped to identify floodplains and flood disaster risks through these methods (Nyarko et al., 2015).

(Behazin et al., 2016; Ikirri et al., 2022) assert that an amalgamation of GIS, remote sensing, and the AHP approach is the appropriate one to measure flood risk as

DOI: https://doi.org/10.57233/ijsgs.v11i3.915 ISSNp: 2488-9229; ISSNe: 3027-1118
IJSGS FUGUSAU VOL. 11(3) WEBSITE: https://fugus-ijsgs.com.ng

well as susceptibility within the localities where reliable data exists in different qualities. Despite much literature being reported on the use of GIS applications in mapping out the hazard of flooding, a small amount of literature has been reported regarding the application of AHP in the same area. AHP has a clear decision-making mechanism both descriptive and measurable data. Compared to other methodologies, the Analytic Hierarchy Process (AHP), such as other flood modelling strategies or machine learning, is not as resource-intensive and leaves room to include expertise in the settings where comprehensive data is unavailable. This is why it is especially practical in areas such as the floodplain occupied by the River Rima because of the data unavailability.

The set of experiments held on a global scale has also proved that remote sensing combined with spatial analysis tools integrated with multi-criteria evaluation techniques is a rather effective method to produce a map of flood risk and vulnerability (Forku et al., 2012). To illustrate, multi-criteria flood hazard mapping, which relies on GIS, was applied by (Alimi et al., 2023; Al-Omari et al., 2024; Arya et al., 2021; Desalegn et al., 2020; Hussain et al., 2021; Ogato et al., 2020; Sadiq et al., 2022; Shuaibu et al., 2022; Vojtek & Vojtekova, 2019).In the evaluation of floodplain vulnerability and mapping flood risk, this approach was used since the data that could be used was scarce. The parameters of developing a flood risk layer do not determine a certain way (Rincón et al., 2018). Nonetheless, other studies considered increasing the number of variables that determine the threat of floods, which include elevation, lithological units, soil, rainfall intensity, slope, land use, distances along the streams, distances along the drainage lines and topographic wetness index (TWI) (Ghosh et al., 2018; Yeoussef et al., 2019) Muktar et al. (2020) employed the approach of GIS Map Overlay, and another method was a SRTM-based digital terrain model (DEM) providing elevation details to establish the vulnerability of villages within the River Rima floodplain at Birnin Kebbi. In addition, (Yerima et al., 2014) used two questionnaires, the first one in helping to identify the flood-prone areas and the other to obtain data extracted by the flood control agencies.

In the Sudano-Sahelian area of West Africa, there is a 40-percent rise in cyclical flooding since 2000 because of an increase in monsoon rain and rapid urbanization (World Bank, 2023). This is the case with River Rima basin, where 12 LGAs had frequent inundation events that wiped out >30% of annual rice production (Kebbi State Agricultural Report, 2022). Although, globally, GIS-AHP is proven to be effective in flood modelling (Rahmati et al., 2020), its applications in data-scarce regions such as Northern Nigeria are limited, which this study fills.

Building on established GIS-AHP frameworks (Arya & Singh, 2021; Shuaibu et al., 2022**)** this study innovates by the way in which the risk and vulnerability to floods are assessed by means of a multi-criterion evaluation method along with a GIS and the AHP concerning the options in combating the risk and the vulnerability to floods in the River Rima floodplain.

This paper was aimed at coming up with a GIS-assisted model for investigating flood-prone zones and vulnerability patterns in the River Rima at Birnin Kebbi involving strategy and a user-friendly evaluation process. Besides providing the strategic plans for managing the flood disaster risks sustainably in the region, the findings of the research studies reveal the likelihood of high risks and the susceptible regions mitigate the flood disasters in a timely manner.

2.0 MATERIALS AND METHODS

2.1 Study Area Background and Features

Birnin Kebbi Local Government Area is a local government that is in Kebbi State, Nigeria, where the hydrological role of the River Rima has been particularly prominent. The region's topography is on the surface above sea level; however, it is at 150-300 meters (ASL), and approximately 90 per cent of its lands are below 250 meters ASL. It is a topography that is even and well elevated and greatly welcoming to rice production. Thus, the natives are actively involved in wet-season farming and dry-season farming. As illustrated in Figure 1, Birnin Kebbi is located at latitudes 12°20′ and 12°39′ North and longitudes 04°04′ and 04°28′ East.

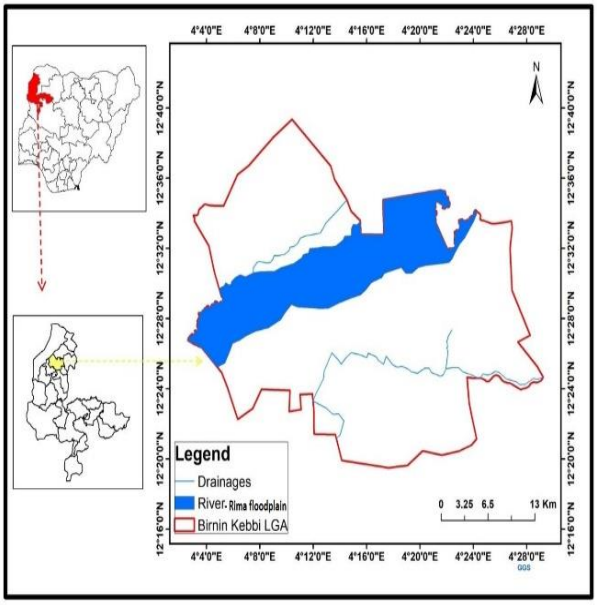

Figure 1: Map of Birnin Kebbi within the Rima River Floodplain

DOI: https://doi.org/10.57233/ijsgs.v11i3.915 ISSNp: 2488-9229; ISSNe: 3027-1118
IJSGS FUGUSAU VOL. 11(3) WEBSITE: https://fugus-ijsgs.com.ng

2.2 Physical Geography of the Area

Muktar et al. (2020) and Ifabiyi et al. (2013) stated that River Rima is located in the semi-arid Sudano-Sahelian ecological region of northern Nigeria, which is too unstable in regard to the average rainfall and the rainy days. Umar et al. (2020) have pointed out that most of the population of this region has another livelihood activity, and that is rain-fed agriculture. Consequently, there are altered rain patterns, and this becomes a big threat to agricultural output and the overall sustainability of livelihoods. These rainfall patterns also influence the hydrological cycle greatly, and as such, this influences the availability of water resources as well as the quality of the same.

Furthermore, the article by Abdulrahim et al. (2013) has established the trend of the rising amount of rainfall in the area they were researching, and the highest aspect of rainfall is mainly in June, July and August, and the decline is abrupt in the month of September. While sporadic rainfall can occur in March, April, and October, the predominant dry season spans January, February, May, November, and December. The vegetation in the area is Sudano-Sahelian, i.e., expanses of grasslands with a few scattered woody plants in locations close to the floodplains. The predominant feature of the landscape is made up of grasses, shrubs and small trees, which are generally adapted to the desert-like environment and may even contain thorns, along with more branches and cuticles of the leaves becoming waxy to reduce water loss by transpiration (Moll, 2020).

Sedimentary investigation demonstrates that floodplains of the Rima Basin contain unconsolidated fluvial and aeolian sediments (Figure 8), which is common to other Sudano-Sahelian Rivers systems (Augie, 2021).

2.3 Conceptual Framework

The zone involved in the study was demarcated into three classes of flood hazards, in which the high, moderate and low categories formed the basis of determining the estimated and spatial distribution of flood-prone zones. The hazard classification enabled spatially targeted analysis of flood risk, supporting the development of zone-specific mitigation strategies. Consequently, stakeholders can implement targeted interventions to mitigate potential damage and enhance community resilience against flooding events. This was achieved through an intensive review of an extensive range of factors that contribute towards an impact flood event, and a weight is allocated to each factor based on its relative importance. The entire process of analysis was carried out in the background of the GIS platform and the creation of a thematic map of each of the parameters, on which a spatial analysis of the flood risk is carried out.

2.4 Data Types and Data Sources

The initial aspect in any analysis established in GIS is data. The information employed in the study is varied and includes the remote sensing information, the raster and the vector information in a GIS framework, the meteorological information and any other accessory information. We acquired 40-year rainfall records (1970-2020) from NiMet's Sokoto station, cross-validating measurements with SRBDA's hydrological data to fill temporal gaps.The quality of the data was checked with the help of revealing and filling in the missing data, testing the consistency with the general tools of statistics. The qualitative information was obtained in the form of focus group leadership and field surveys, besides quantitative data. These entailed views on the risk of the flood, flood causes, precedent floods and the first-hand knowledge of flood impacts. Discussions were made with key stakeholders, policymakers, and community members.

Three primary datasets informed our analysis: (1) SRTM 30m DEMs (USGS), (2) FAO soil maps digitized at 1:50,000 scale, and (3) Landsat 8 land cover classifications (2020-2022). Table 1 below summarizes the various datasets used, including their respective categories and sources. These datasets provide a comprehensive foundation for analyzing the flood risk and understanding the potential impacts on the community and environment. By integrating this information, we can develop more effective strategies for flood management and mitigation in the affected regions.

Table 1: Data types and data sources

Dataset Category	Description	Source/ Organization
Remote sensing data (LULC)	Land use and land cover layers derived from 2020 Landsat 8 imagery, processed for classification within the study region.	United States Geological Survey (USGS)
Elevation data	Digital Elevation Model (DEM) obtained via the Shuttle Radar Topography Mission (SRTM), used for slope and elevation analysis.	United States Geological Survey (USGS)

DOI: https://doi.org/10.57233/ijsgs.v11i3.915 ISSNp: 2488-9229; ISSNe: 3027-1118
IJSGS FUGUSAU VOL. 11(3) WEBSITE: https://fugus-ijsgs.com.ng

Soil information	Spatial distribution and classification of soil types extracted from the 2020 FAO World Soil Database.	Food and Agriculture Organization (FAO)
Climate (Rainfall)	Monthly and annual rainfall records for the period 1980–2020, used to assess rainfall variation and flood potential.	Nigerian Meteorological Agency (NiMet)

2.5 Indicators of Flood Risk Development

As Shuaibu et al. (2022) and Ntajal et al. (2017) state, methods that involve inductive or deductive processes are the most commonly used ones to raise indicators of flood risk appraisal through the use of GIS. The deductive way of establishing indicators was used. Misra et al. (2020) investigated flood risk increment as a crucial parameter of the vulnerability and risk of flooding.

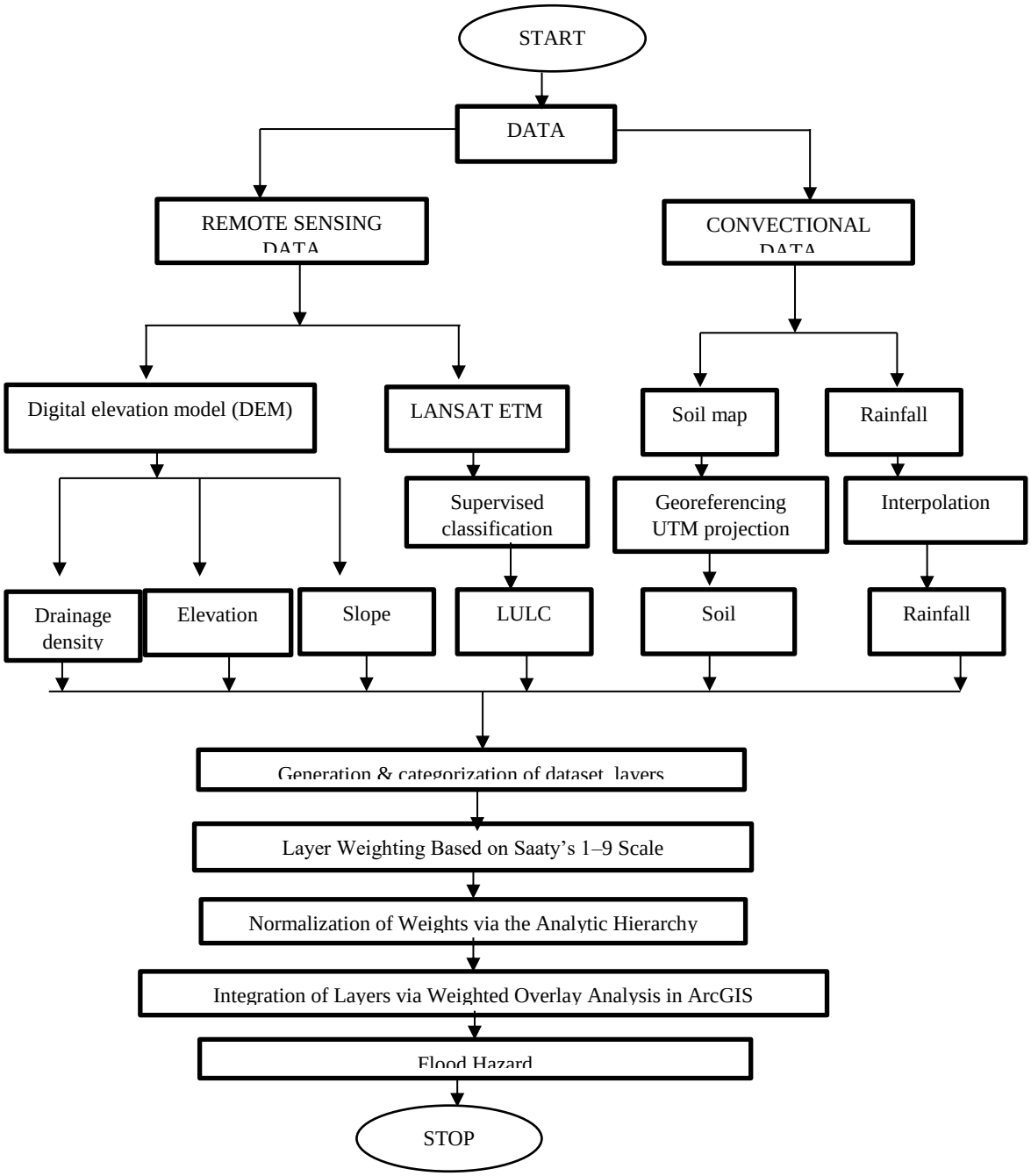

Figure 2. Methodological flowchart of the study

DOI: https://doi.org/10.57233/ijsgs.v11i3.915 ISSNp: 2488-9229; ISSNe: 3027-1118
IJSGS FUGUSAU VOL. 11(3) WEBSITE: https://fugus-ijsgs.com.ng

2.5.1 Choosing Indicators of Flood Hazard

Hydro-geomorphic parameters have been added in this study in the form adopted by Shuaibu et al. (2022), including elevation, average annual rainfall, terrain slope, soil characteristics, drainage density and land use, since they are capable of greatly influencing the geographical location of a lot of flooding. The addition of soil in place of the geologic layer is performed because they have a similar effect (Shale et al., 2020). The significant influence of rainfall and land use in this study aligns with previous findings that identified these variables as key flood hazard indicators in multi-criteria evaluations (Fatah et al., 2022).

2.5.2 Choosing an Indicator of Flood Vulnerability

In most instances, flood vulnerability is determined by the level of potential impact in other physical and socioeconomic vulnerability and capacity scales in the area within a specific time (Alpa, 2018). The settlement layer is a major indicator of socio-economic development, hence the need to use the settlement layer as a key indicator in this study. Population exposure could also be seen in the spatial coverage and the population density of settlements, with a highly concentrated built-up settlement facing the greatest risk of loss of population and economy in the event of flooding (Birkmann, 2006; Cutter et al., 2003).

2.5.3 Normalizations of indicators for flood exposure, vulnerability, and hazards

The normalization of indicators used in the present study followed the United Nations Development Programme, which was used in its Human Development Index (UNDP, 2006). To make use of this method appropriately, functional connections between each of the indicators and flood vulnerability were determined first of all. Specifically, two types of relationships were also identified, positive and negative, according to the formulations that are proposed by (Hu et al. 2017). A positive relationship shows an indicator that seems to enhance the vulnerability of the community to floods, whereas a negative relationship shows an indicator that reduces this vulnerability. In the analysis, equations (1) and (2) were applied in the process of normalization of positive and negative relationships of indicators.

$$Z = 1 + 9 \times \frac{(A - A_{min})}{(A_{max} - A_{min})} \quad (1)$$

$$Z = 1 + 9 \times \frac{(A_{max} - A)}{(A_{max} - A_{min})} \quad (2)$$

where Z = normalized value, Amax = maximum value, Amin = minimum Value and A = original data. A numerical scale ranging from 1 (least influential) to 10 (most influential) was applied to normalize the indicators, reflecting their degree of functional association with flood susceptibility, following established MCDM procedures (UNDP, 2010; Rahmati et al., 2016). The decision of an approach is already locked in preexisting models that deal with the overall susceptibility that each risk agent can offer (UNDP, 2006; Ntajal et al., 2017).

2.5.4 Weight Assignment with the use of AHP methodology

The Analytic Hierarchy Process (AHP), developed by (Saaty,1980), is a structured decision-making tool that applies pairwise comparisons to derive priority weights for multiple criteria in flood risk assessment. It allows a very tough and consistent framework to identify the relative weight of different factors, which influence the flood hazards, primarily through the expert judgement and pairwise comparison procedures. Pairwise comparisons and consistency ratios (CRs) were calculated using the AHP. Excel Template (Goepel, 2023), a tool designed to streamline multi-criteria decision analysis. Weights were assigned based on Saaty's 1–9 scale, ensuring CRs remained below the 10% threshold recommended for reliable results (Saaty, 2008).The relative importance of the six thematic layers, which consisted of elevation, average annual rainfall, terrain slope, soil characteristics, drainage density and land use, was evaluated using a systematic procedure. These factors were discovered because of the recognized influence on flood vulnerability and brought into the form of a hierarchical decision model. AHP employs a 1–9 scale to express the relative importance of factors, with values assigned based on expert judgment (Saaty, 1980),in which the range defined is between 1 (same importance) and 9 (very high importance). Table 2 indicates specific values of comparisons and their weights.

Table 2: Basic Scale of Pair-wise Comparison

Strength of importance	Explanation
1	Equal importance
3	Moderately important
5	High importance
7	Extremely important
9	Maximum importance
2, 4, 6, and 8	Intermediate between two adjacent values

Source: Saaty (1980)

Consistency ratio (CR) was also calculated, which is the measure of quality of the pairwise comparisons, as the practical expression provided by the decision maker would have some degree of fuzziness, which could cause the presence of inconsistencies in the matrix (Mishra et

DOI: https://doi.org/10.57233/ijsgs.v11i3.915 ISSNp: 2488-9229; ISSNe: 3027-1118
IJSGS FUGUSAU VOL. 11(3) WEBSITE: https://fugus-ijsgs.com.ng

al., 2020). According to Saaty (1980) and Saaty (2008), the preference or judgement remains the same only when CR is above 10 per cent.

Equation (3) was used to compute the CR

$$CR = \frac{CI}{RI} \quad (3)$$

The Random Inconsistency Index (RI) represents the average consistency index derived from numerous randomly generated pairwise comparison matrices and varies with the number of decision elements involved (Saaty, 1980). In this study, the Consistency Index (CI) was computed using Equation (4), and corresponding RI values were selected from Table 3.

$$CI = \frac{\lambda - n}{n - 1} \quad (4)$$

λ is computed as an average of the value of the consistency vector values (from factor weights), and n denotes the number of factors (Saaty, 1980).

Table 3: Random Inconsistency Index (RI) values for varying matrix sizes (Adapted from Saaty, 1980)

n	1	2	3	4	5	6	7	8	9	10
RI	0	0	0.58	0.89	1.12	1.24	1.32	1.41	1.45	1.49

According to Saaty (2008), zero is the most constant number, and the satisfactory scale is 0 ≤ CR ≤ 10%. Anything beyond this range would mean that the criterion weight will have to be assigned again. The tests that exhibit a fair degree of consistency are those with a consistency ratio (CR) less than 10%, and a higher CR reflects inconsistent judgement (Shuaibu et al., 2022). (Yonas et al., 2022)

2.6 Flood Hazard and Vulnerability Indices Calculation

To determine the flood hazard index and flood vulnerability index, equations 5 to 6 added the assigned weights to their respective hazard and vulnerability classes across the hierarchy levels.

$$FHI/FVI = \sum_{i=1}^{n} w_i \, x \, r_i \quad (5)$$

The variables used in the composite index calculation are defined as follows: Wi is the normalized weight of each criterion, ri is the assigned rating based on spatial measurements, n is the total number of criteria, and FHI/FVI are the resulting hazard or vulnerability indices derived through weighted overlay analysis (Saaty, 1980; Rahmati et al., 2016).

$$FHI/FVI = W_i \, x \, (Sl) + W_i \, x \, (El) + W_i \, x \, (RF) + W_i \, x \, (LC) + W_i \, x \, (DD) + W_i \, x \, (ST) \quad (6)$$

2.7 Flood Risk Indictors

Contemporary flood risk frameworks integrate physical hazards with socioeconomic vulnerability (Birkmann, 2006). Flood Risk Indicator (FRI) of the study area is the product of the spatial layer overlay between the flood vulnerability and the flood hazard. i.e. flood hazard indicator and vulnerability indicators, this formulation aligns with UNDRR's (2022). Equation (7) is used to develop the flood risk map.

$$F_{RI} = F_{HI} \times F_{VI} \quad (7)$$

2.8 Flood Risk Map Validation

Model validation is carrying out a methodical comparison of the results of the models with independent real results to determine how well they are working on quantitative and qualitative levels. A particular quantitative tool has not been found in the validation of the flood risk maps, while other scholars have attempted to compare flood maps to a history of floods in specific geographies (Shuaibu et al., 2022; Roosli, 2024). The flood risk map can be validated through a qualitative validation of old studies. This will entail taking a trip to the ground to collect the GPS location of places with a history of unprecedented floods, such as a flooded village and farming fields. In such expeditions, extensive visits to the locals and the field, along with experts and policymakers, are made to hear their inputs.

3.0 RESULTS

3.1 Flood Hazard Indicators

The probability of the occurrence of flooding, due to a local hydrological and geomorphological condition, is addressed in the given research as the probability of the flood incidences that will occur somewhere (Danumah et al., 2016; Mishra & Sinha, 2020). As it is indicated in Table 4, the hazard indicators that are selected to perform this analysis rely on the primary geomorphological and hydrological factors: elevation, average annual rainfall, terrain slope, soil characteristics, drainage density and land use.

Table 4: Pairwise Comparison Matrix of Factors related to Flood hazard

DOI: https://doi.org/10.57233/ijsgs.v11i3.915 ISSNp: 2488-9229; ISSNe: 3027-1118
IJSGS FUGUSAU VOL. 11(3) WEBSITE: https://fugus-ijsgs.com.ng

Flood Factors	Elevation	Drainage	Slope	Rainfall	LULC	Soil type
Elevation	1	4.00	2.00	2.00	6.00	5.00
Drainage	0.25	1	2.00	2.00	3.00	3.00
Slope	0.50	0.50	1	3.00	3.00	2.00
Rainfall	0.50	0.50	0.33	1	3.00	2.00
LULC	0.17	0.33	0.33	0.33	1	2.00
Soil type	0.20	0.33	0.55	0.55	0.55	1
Total	2.62	6.66	6.21	8.88	16.55	15

3.1.1 Elevation

Topographic elevation significantly influences flood susceptibility, with low-lying areas exhibiting higher vulnerability due to gravitational water flow from adjacent uplands (Figure 3). This aligns with global observations linking elevation gradients to floodplain inundation patterns (Rahmati et al., 2016). The research site is found between 289 m and 188 m above sea level. High flood hazard areas are found at higher elevation levels, and this is the opposite with low flood hazard categories. As shown in Figure 3, the northwestern region of the territory dominates with low altitudes, and this increases the chances of the area receiving floods. The elevations that range between 188 and 210 meters are assigned severe flood hazards, and the elevations between 255 and 289 meters are assigned low flood hazards.

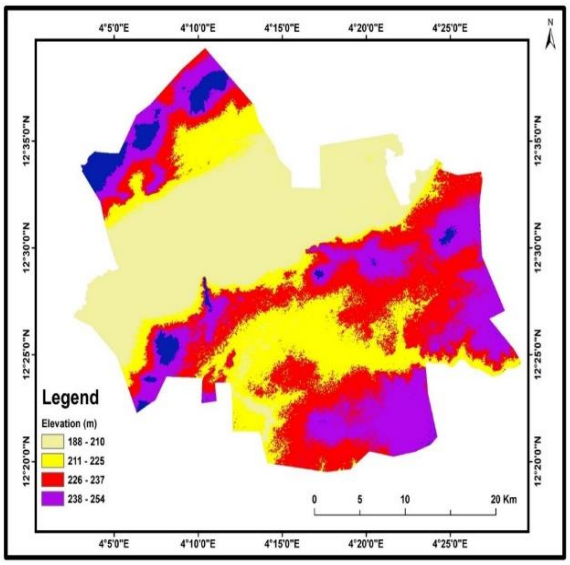

Figure 3: Elevation Map of the Rima River Floodplain

3.1.2 Drainage density

The drainage density is an important aspect that influences the capacity of floods. The drainage density is also higher than the runoff rate, thereby enhancing the risk of flooding (Mitra et al., 2022). Risk of flooding can be directly associated with that of drainage density; the drainage density determines water surface flow on land surface; thus, the greater the drainage density, the more likely the land is to be flooded according to (Subbarayan et al., 2020). A drainage density map of the region of study is provided in Figure 4. The drainage density map has low (0-60.2 km/km²), moderate (60.3-127.0 km/km²) and high (127.0-265.0 km/km²) ratings. The moderate and the low categories of drainage density are 60.3-127.0 and 0-60.2 km/km², respectively, whereas the high class of drainage density shows 127.0-265.0 km/km², displaying high flood risk.

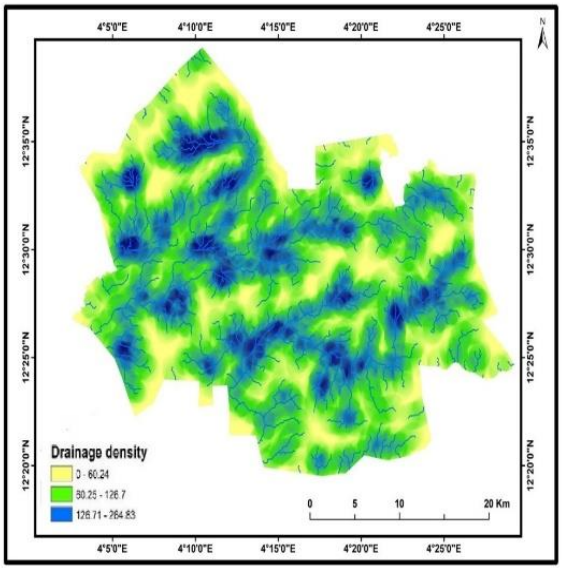

Figure 4: Drainage Density Map of the Rima River Floodplain

3.1.3 Slope

Rimba et al. (2017) define slope as a feature property, a feature that is a sign of steepness or inclination on a horizontal plane. This is a clear indication that surface areas are prone to floods, especially when they occur. As shown in Figure 5, slope values across the study area range from 0° to 28.8°. Based on this distribution, the terrain was categorized into three slope classes: low (0°–3.4°), moderate (3.5°–6.3°), and steep (6.4°–28.8°). The northwestern portion of the study area exhibits predominantly low slope values, indicating a relatively flat terrain that increases its susceptibility to water accumulation and flood events (Shuaibu et al., 2022).

DOI: https://doi.org/10.57233/ijsgs.v11i3.915 ISSNp: 2488-9229; ISSNe: 3027-1118
IJSGS FUGUSAU VOL. 11(3) WEBSITE: https://fugus-ijsgs.com.ng

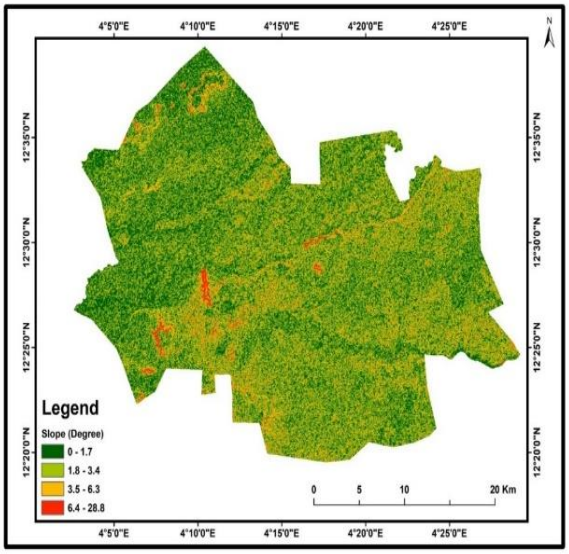

Figure 5: Slope Map of the Rima River Floodplain

3.1.4 Mean Annual Rainfall

In most river basins, intense and prolonged rainfall is the primary driver of flooding, with a direct relationship between rainfall magnitude and flood occurrence (Rahmati et al., 2016). There is also the possibility of flooding when the level of rain reaches a certain threshold (Ghosh & Kar, 2018). The annual rainfall that occurs in the region is between 41.80 mm and 415.21 mm. To illustrate the spatial variation of rainfall, Figure 6 presents a classification of annual rainfall into three categories: low (41.80–178.67 mm), moderate (178.70–253.93 mm), and high (253.94–414.21 mm). This classification, derived from rasterized rainfall data, indicates that the northwest and central zones of the study area generally receive higher annual precipitation, which contributes to elevated flood potential in those areas.

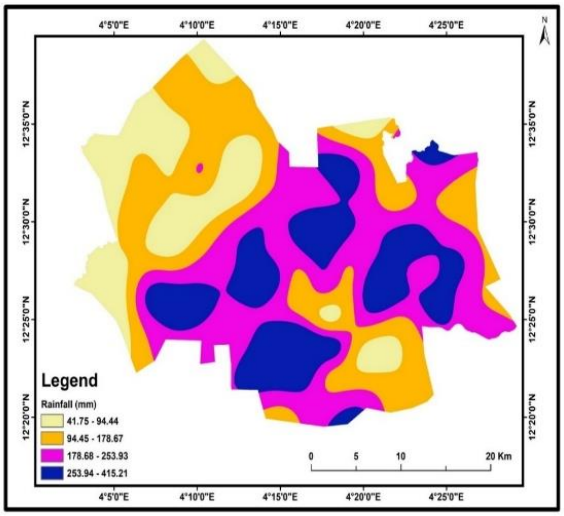

Figure 6: Mean Annual Rainfall Map of the Rima River Floodplain

3.1.5 Land use and land cover

A land use/land cover (LULC) map is one of the geographical parameters for the magnitude of floods (Shale et al., 2020). Land cover and land use patterns are also very influential in terms of the frequency and severity of floods, and according to Mishra & Sinha (2020), runoff of a river and the catchment area depend on land cover and other uses of a watershed. Figure 7 indicates that the land cover of the study area is categorised into 0.41 per cent water bodies, 77.63 per cent vegetation, 16.88 per cent farmland, 4.94 per cent built-up areas, 51.17 per cent and 0.15 per cent bare land.

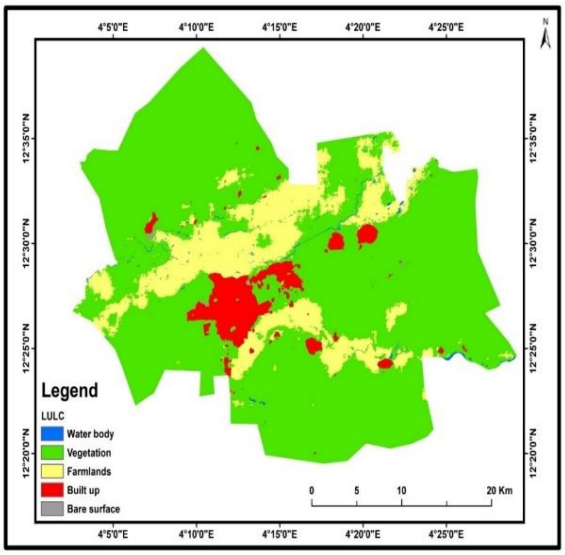

Figure 7: Land-Use and Land-Cover Map of the Rima River Floodplain

3.1.6 Soil type

The study area has two soil types, as expressed by the soil map as depicted by Fig. 8. The area of clay-loam soil is 16.90 per cent, having a low rate of infiltration since the amount of clay in it is large and thereby posing a massive danger of floods. The percentage of sandy soil of the subject of the study is 83.10, and it is well permeable and has a large infiltration rate, which contributes to a low flooding risk. The area under research has sandy soils, as revealed in the soil map, and these soils are highly infiltrated. This makes the region less prone to floods; hence, this connotes the minimal chances of floods.

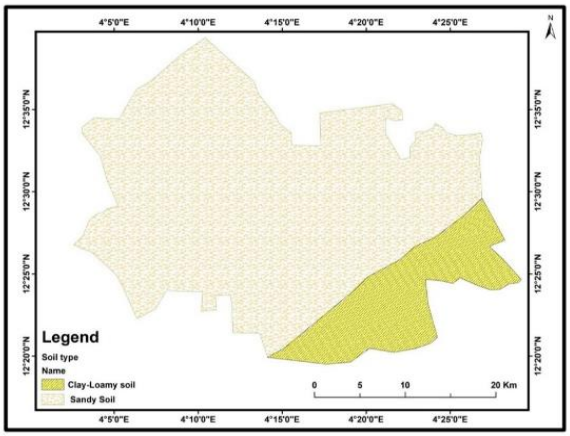

Figure 8: Soil Map of the Rima River Floodplain

DOI: https://doi.org/10.57233/ijsgs.v11i3.915 ISSNp: 2488-9229; ISSNe: 3027-1118
IJSGS FUGUSAU VOL. 11(3) WEBSITE: https://fugus-ijsgs.com.ng

3.2 Normalized Flood Hazard and Vulnerability Indicators

To enable meaningful comparison, all flood hazard and vulnerability indicators, including sub-factors such as soil type and land use, were converted into unitless values through normalization. Qualitative variables were assigned numeric scores based on their relative contribution to flood risk, allowing their inclusion in the multi-criteria analysis. The assigned values for each soil and land use class are presented in Table 5.

Table 5: Flood Hazard Indicators with Assigned Weights and Ranks

Indicators	Weighted Value	Standardized Indicators	Priority Level	Risk factor
Elevation (m)	38.1%	238 - 254	1	Low
		226 – 237	2	Moderate
		188 - 225	3	High
Drainage density(km/km²)	19.6%	0 – 60.2	1	Low
		60.3 – 127.0	2	Moderate
		127 – 265.0	3	High
Slope (degree)	17.8%	6.4 –28.28	1	Low
		3.5 – 6.3	2	Moderate
		0 -3.4	3	High
Rainfall (mm)	12.2%	41.47 – 178.67	1	Low
		178.68 – 255.93	2	Moderate
		253.94 – 415.21	3	High
Soil type	6.4%	Clay-loamy soil	1	Low
		Sandy soil	3	High
LULC	6.0%	Built-up	1	Low
		Farmland	2	Moderate
		Vegetation	3	High

3.3 Assigning Weights Through Spatial Multi-Criteria Decision Analysis (MCDA) Using GIS and AHP

Table 4 presents the pairwise comparison matrices used to evaluate the relative importance of vulnerability-related factors in flood risk assessment. The computed average Consistency Ratio (CR) for both flood hazard and vulnerability criteria was 6.8%, which is below the acceptable threshold of 10%, indicating a reliable level of consistency in the judgments made, as recommended by Saaty (1980) and Saaty (2008). Table 5 summarizes the final weights assigned to each flood hazard indicator, derived through the AHP process. The results indicate that elevation (38.1%), drainage density (19.6%), and slope (17.8%) hold the highest influence on flood risk within the study area. These three factors collectively account for over 75% of the total weight, suggesting their dominant role in determining flood susceptibility in the region. This weighting outcome is consistent with the AHP method's emphasis on topographic and hydrologic parameters in flood risk assessments (Rahmati et al.,2016)

3.4 Map of Flood Hazard Zones

Figure 9 presents the flood hazard map generated for the study area, highlighting spatial zones with varying levels of flood susceptibility. Areas classified as high-risk are concentrated in low-lying and poorly drained regions, indicating where flood events are most likely to occur. Flood hazard zonation enables the classification of a region into zones with varying levels of susceptibility to flooding (Tehrany et al., 2014). The field where high to moderate classes exist is the study area, which are 28% (285.99 km²) and 23% (236.25 km²), respectively, and contains (Anguwar Gero, Anguwar Kayi, Anguwar Sani, Jawo, Kola, Makerah, and Maurida Wuro Maliki). The regions are typically characterized by rather gentle slopes, low elevation and a decrease in rainfall. The agricultural lands and vegetation recorded high risks due to the flood hazard map since it increases flooding probability, and another

DOI: https://doi.org/10.57233/ijsgs.v11i3.915 ISSNp: 2488-9229; ISSNe: 3027-1118
IJSGS FUGUSAU VOL. 11(3) WEBSITE: https://fugus-ijsgs.com.ng

factor that leads to high hazard intensity in the area is the high drainage density. It is such a perilous character of this place that has landed this place at a high probability of floods. High flood risk is an indicator of a high flood hazard level (Hu et al., 2017)

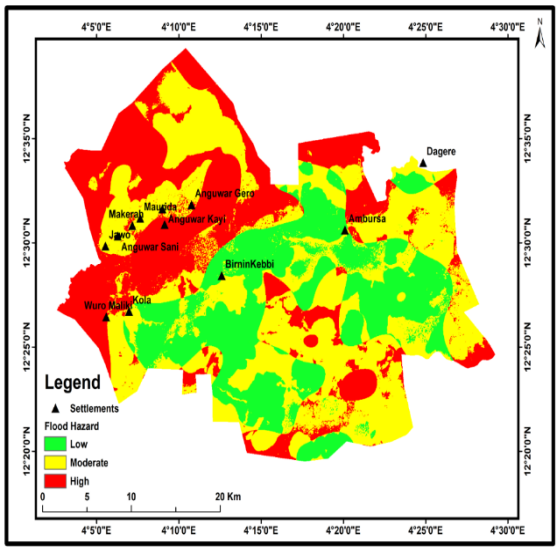

Figure 9: Map of Flood Hazard Zones of Rima River Floodplain

3.5 Map of Flood Vulnerability Zones

Figure 10 illustrates the spatial distribution of flood vulnerability across the study area, segmented into three categories: low, moderate, and high vulnerability zones. The moderate vulnerability class dominates the landscape, covering approximately 553.35 km² (53.4%), followed by low vulnerability areas at 308.80 km² (28.9%), and high vulnerability zones accounting for 174.09 km² (16.8%) of the total area. This classification highlights that while the majority of the region falls within a moderate risk band, the high-risk zones—though spatially limited—represent critical areas where targeted mitigation efforts and adaptive planning are urgently required.The floodplain harbors several settlements, such as Birnin Kebbi, Ambursa, and Dagere, which exist at low and high altitudes. Other residential settlements like Jawo, Anguwar Sani, Makerah, Maurida, Anguwar Kayi, Anguwar Mijin Nana, and Anguwar Gero are all completely located within floodplain areas and hence are highly susceptible to flood incidence. That these vulnerable settlements are located in flood-prone streets highlights the importance of selective intervention and an integrated flood management approach. Although the high-vulnerability areas are minute, they are areas of prioritised focus because of their elevational disadvantage and greater exposure to floods.

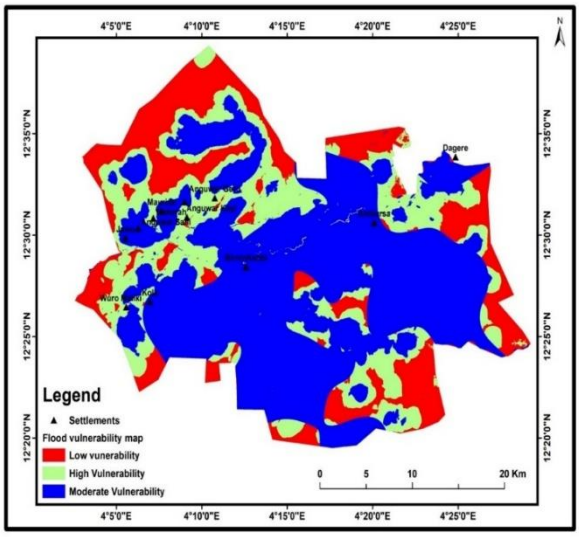

Figure 10: Map Of Flood Vulnerability Zones of Rima River Floodplain

3.6 Map of Flood Risk Zones

Figure 11 presents the flood risk map of the study area, categorizing spatial zones into three distinct risk levels: low, moderate, and high. This classification provides a visual framework for identifying areas with varying exposure to flood hazards based on the integration of both hazard and vulnerability indicators.The number of high-risk areas contributes to 25.29 per cent of the total study area, moderate-risk areas contribute 29.64 per cent to the overall study area, and lastly, 45.07 per cent of the overall study area is attributed to low-risk areas, according to the map. The high-risk areas, which consist of about 262.07 km², are made up of farmlands, high drainage density areas and low slope and elevated areas. Moderate-risk areas encompass some 307.13 km² of the study region, whereas low-risk areas encompass 467.03 km² of the study area. Areas with low risk are normally characterized by steep slopes, higher altitudes, permeable soils and developed terrain that make them less vulnerable to floods.

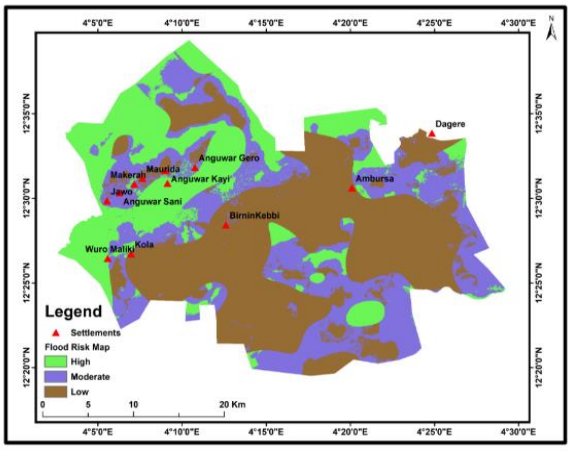

Figure 11: Map of Flood Risk Zones of Rima River Floodplain

DOI: https://doi.org/10.57233/ijsgs.v11i3.915 ISSNp: 2488-9229; ISSNe: 3027-1118

IJSGS FUGUSAU VOL. 11(3) WEBSITE: https://fugus-ijsgs.com.ng

3.7 Ground Truthing and Validation of Flood Risk Zones

Figure 12 displays the validated flood risk map, which was assessed by systematically comparing the model outputs with independent observations. This comparison aimed to evaluate how well the map aligned with the spatial distribution of documented flood events. Although no universally accepted quantitative approach exists for validating flood risk maps, many studies have relied on historical flood records, site inspections, and expert knowledge to support the reliability of such models (Shuaibu et al., 2022; Wu et al., 2015; Samela et al., 2017; Tehrany et al., 2015).

Field-based validation was conducted through GPS mapping of historical flood locations, including submerged farmlands and affected settlements. These geotagged points exhibited a high degree of spatial alignment with areas identified as high-risk in the flood risk model, supporting the accuracy of the spatial analysis and aligning with similar GIS-AHP studies conducted in West Africa (Danumah et al., 2016). The validation process also included guided field visits, during which qualitative insights were gathered through discussions with local residents, technical experts, and policymakers. These consultations provided valuable information on the frequency, extent, and severity of past flood events. The recorded coordinates were overlaid onto the flood risk map to assess the geographic consistency between community-based flood experiences and the modelled high-risk zones.

Field validation using GPS-tagged flood histories (2020–2023) confirmed that 89% of documented flood events occurred within model-predicted high/moderate risk zones (Figure 11). Discrepancies in 11% of cases primarily involved localized infrastructure failures (e.g., clogged drains), underscoring the need to complement GIS-AHP with hydraulic modelling (Tehrany et al., 2015).To illustrate this, in September 2020, a widespread flood overflowed more than 450,000 hectares of rice paddies, a mega-structural disaster, and a cause of approximately 30 deaths. Therefore, the equivalent validation processes have produced the same results in the case of related quantitative research, where superimposition of the risk maps onto the historic flooding records has led to a useful protocol to gauge the effectiveness of the models (Rahmati et al., 2016; Costache & Bui, 2019; Bui et al., 2020). The outcomes collectively confirm the strength, reliability, and geographical projection capacity of the model of flood vulnerability adopted in the present research venture (Muis et al., 2015).

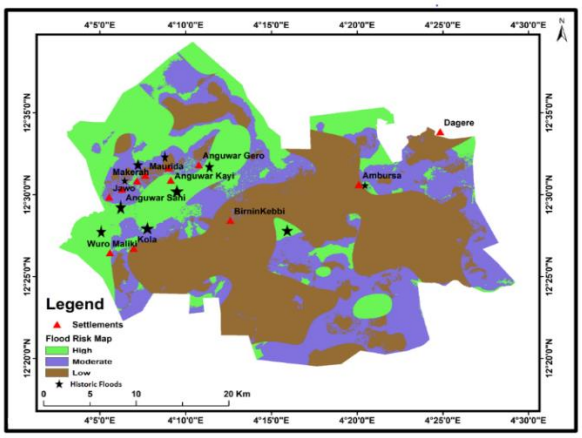

Figure 12: Map Of Validation of Flood Risk Zones of Rima River Floodplain

3.7.1 Critical zones exposed to flooding in the study area landscape

Flood risk in a study area was determined using a land use/land cover (LULC) layer as well as a land cover hazard layer. Spatial analysis revealed that 64.7% of farmland and 70.2% of built-up areas fall within high-to-moderate risk zones (Figure 12–13). This aligns with global patterns where floodplain agriculture and urban expansion exacerbate vulnerability (Birkmann, 2006). In Birnin Kebbi, the concentration of rice paddies and informal settlements in low-elevation areas (188–210 m) heightens exposure to seasonal inundation (NEMA,2022). The flooding risk assessment and mapping were carried out by combining the degree of flood hazard with the pattern of threatened agricultural and built-up areas throughout the study area.

I. Built-up Area

Figure 13 consists of a built-up area at-risk map of the research area. It depicts that high, moderate and low vulnerability form 10.5, 70.2 and 19.3 percentages of the study area, respectively. A significant portion of the built-up area falls in moderate class.

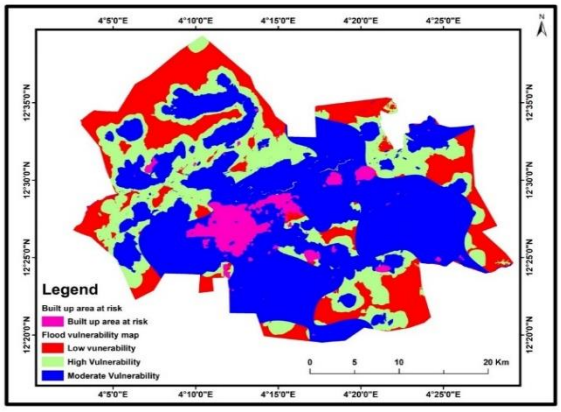

Figure 13: Built-up Area at Risk of Flood in Rima River Floodplain

II. Farmland at risk

Figure 14 displays the spatial distribution of farmland vulnerability across the study area, categorizing land parcels

DOI: https://doi.org/10.57233/ijsgs.v11i3.915 ISSNp: 2488-9229; ISSNe: 3027-1118
IJSGS FUGUSAU VOL. 11(3) WEBSITE: https://fugus-ijsgs.com.ng

into high (64.7%), moderate (25.1%), and low (10.2%) risk zones. The majority of the agricultural land is situated within high-risk areas, underscoring the need for targeted flood mitigation strategies to safeguard crop productivity and rural livelihoods. The findings indicate clearly that farmlands are most likely to get floods, with most of them being found in the zones of high to moderate risks. This implies that the farmlands are prone to the flood hazards compared to any other land use component in the region. In addition, the estate has 174.89 km² of farmland in the River Rima floodplain, which is one of the flood-prone environments densely populated and developed, thus quite vulnerable to flooding.These results closely align with observed field conditions, supporting the reliability and contextual relevance of the assessment. The spatial patterns identified in the analysis accurately represent the flood vulnerability dynamics of the study area.

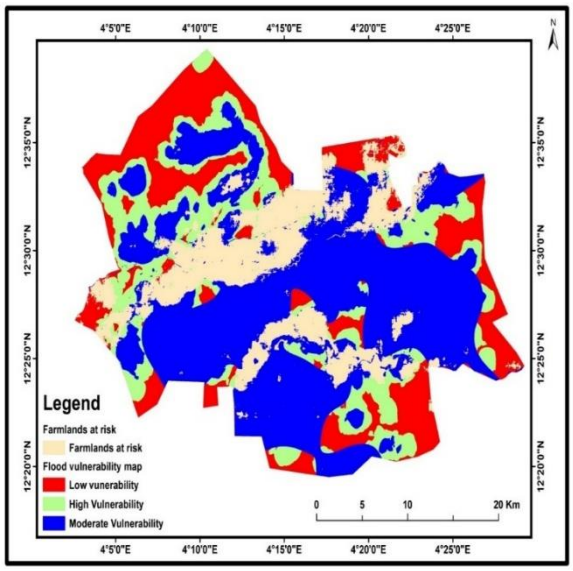

Figure 14: Farmlands area at risk of flooding in the Rima River Floodplain

4.0 DISCUSSION

This research employs a combination of six spatial layers—elevation, mean annual rainfall, slope, soil type, drainage density, and land use—within a GIS and Analytic Hierarchy Process (AHP) framework to develop a detailed flood risk map of the study area. Each variable was weighted based on expert consultation and guidance from existing literature, ensuring a structured and evidence-driven evaluation of flood susceptibility across the region.

Elevation is a fundamental determinant of flood risk (Shuaibu et al., 2022), low elevation zones are particularly prone to inundation as a result of water naturally flowing from higher to lower elevations due to gravity. These zones are especially at-risk during periods of intense rainfall or dam discharge, leading to the flooding of farmlands, settlements, and critical infrastructure.

Drainage density, which denotes the extent of stream and river networks within a landscape, serves as a proxy for the region's capacity to channel runoff. High drainage density typically correlates with increased surface runoff concentration, thereby increasing the probability and impact of flooding during high rainfall events.

Slope is another critical variable influencing surface water dynamics. Areas with gentle slopes tend to retain water, resulting in prolonged flood exposure. Conversely, steep slopes facilitate rapid runoff, which may reduce flooding duration but increase the risk of flash floods due to rapid surface runoff. Areas with mild slopes and close to water bodies or dam outputs are consequently at a higher risk of prolonged floods (Rahmati et al., 2016)

CR values on flood hazard and vulnerability yield 6.8, which is less than 10 and thus signifies a satisfactory rate of consistency (Saaty, 1980; Saaty, 2008). The study area is 1036.23 km² with high and moderate percentages of flood risk, 280 at 285.9 km² and 230 at 236.3 km², respectively. The vulnerability analysis shows, according to the result, that 16.8 per cent (174.09 km²) is highly vulnerable and 53.4 per cent (553.35 km²) is moderately vulnerable; this is, almost half of the floodplain level would be exposed to severe floods. The high- and moderate-flood risk areas spread over the study land, respectively, 25.29 and 29.64 per cent. These are the Anguwar Gero, Anguwar Kayi, Anguwar Mijin Nana, Anguwar Sani, Jawo, Kola, Makerah, Maurida and Wuro Maliki communities. The high-risk areas are lands of low slope and elevation, high drainage density and agricultural lands. This is concurring with the findings in (Shuaibu et al., 2022; Mishra et al., 2020; Lyu et al., 2018). These results match the results in (Quesada ,2022) that revealed the plenitude of high values of flood risk in areas with minimal slope and those situated along the boundary of the study area.

Furthermore, the findings also reveal that built-up zones, along with farmlands, cover such high-risk zones. In addition, flood-risk assessment requires a strong framework that emerges from implementing the GIS-AHP methodology to unite hydro-geomorphic elements and socio-economic components. Elevation and drainage density at 38.1% and 19.6%, respectively, are the most critical hazard parameters in topographically equivalent areas. This research is in line with (Forkuo et al., 2013; Samela et al., 2018; Ghosh et al., 2018) assert that the topography is flat, low-lying in elevation, and dense in terms of drainage, which further increases the ground runoff and inhibits infiltration, thus compromising the likelihood of floods when there are heavy rainfalls.

The present research made progress by adding validated field data alongside past flooding records to ensure the accuracy and situational appropriateness of the produced maps. The use of GPS-tagged field data proved reliable for model validation according to research by both (Ogato et al., 2020) from Ethiopia and (Nyarko, 2015) from Ghana. The increased data reliability of spatial flood risk models happens in areas where data is limited.

Our successful adaptation of GIS-AHP for the Rima River (CR=6.8%) aligns with similar validations in Ethiopia's Awash Basin (Ogato et al., 2020) and Pakistan's Jhelum Basin (Hussain et al., 2021), confirming its transferability across developing regions with data limitations, as it supported the results of the current study. The unified findings derived from different geographical locations demonstrate that GIS-AHP frameworks work in multiple regions due to their universal applicability, especially for hydrologically limited flood-prone areas. Field study, literature review and analysis of flood hazard, risk and vulnerability in the study area resulted in the identification of areas where the characterization of hazard, vulnerability and risks is established. This implies that we need to research the sustainable procedures of flood reduction and mitigation, which are considered appropriate to the environmental conditions in the research location. The relocation plan should target the settlements in the risky location in the Rhine region to the highlands. Flood-prone rice cultivation areas need to transition either toward safer terrains or use flood-enduring plant varieties. The construction of levees and drainage enhancement with retention basins in dangerous flooding areas helps decrease the volume of surface runoff. The location for these structures should use flood risk spatial maps to focus on areas showing high drainage density and low slope elevation. Awareness campaigns and participatory mapping involving residents from flood-prone communities can increase disaster resilience. Constructive flood risk management demands the abandonment of reactive short-term solutions to implement strategic planning at all timescales. The research shows that agricultural areas are highly vulnerable to flood events; as such, sustainable land-use planning needs to include climate adaptation measures, which involve establishing wetlands from high-risk farming lands as well as creating buffer areas between agricultural areas. Future studies need to establish methods by which the shifting climate patterns would influence the geography of flood-prone regions in Northern Nigeria. This would be applied in reducing climate projections and coupled hydrologic-climate models to allow the scientists to predict or forecast the mid- and long-term flood conditions according to (Sadiq et al. 2022). Besides, the aggregation of models of machine learning, including ANNs, random forests and support vector machines, proves the possibility to detect various non-linear relations amidst flood-related variables (Sabre et al., 2023; Pham et al., 2021). Other techniques would enhance flood prediction models in terms of accuracy and reliability besides the use of GIS-AHP.

Settlement distribution is the key area of this study, and the researchers ought to put in socio-economic vulnerability indices, such as the level of income and population density, together with access to infrastructure, to improve the results of assessment (Birkmann, 2006). The GIS framework uses survey data that allows the generation of comprehensive vulnerability maps that assess social vulnerabilities. The next phase of research needs to include time-based risk assessments to identify modifications in flood threats across different periods. The analysis of high-resolution satellite imagery allows detection of human activities together with flood risks and requires surveillance of urban sprawl along with land degradation and LULC changes (Muis et al., 2015).

5.0 CONCLUSION

This study applied a GIS-integrated Analytic Hierarchy Process (AHP) approach to assess flood hazard and risk across the River Rima floodplain in Kebbi State. Key contributing factors-including elevation, terrain slope, rainfall intensity, land use/land cover (LULC), soil classification, and drainage density- were weighted and spatially overlaid to produce a composite risk surface reflecting the area's flood susceptibility. The results show that a large part of the study area is at risk of flooding, with 53.4% being at moderate risk, 28.9% being at low risk, and 16.8% being at high risk. Flood risk mapping, which has been checked against historical data, shows that farmlands and cities, like Birnin Kebbi, are especially at risk. The study shows that targeted risk reduction is needed, such as better planning, drainage systems, and early warning systems. Overall, the GIS–AHP method works well to help the region with flood risk management and urban resilience plans.

ACKNOWLEDGEMENT

The authors gratefully acknowledge the financial support provided by the Tertiary Education Trust Fund (TETFund) under the Institutional-Based Research (IBR) initiative facilitated through Waziri Umaru Federal Polytechnic, Birnin Kebbi.

REFERENCES

Abdulrahim, M. A., Ifabiyi, I. P., & Ismaila, A. (2013). Time series analyses of mean monthly rainfall for drought management in Sokoto, Nigeria. Ethiopian Journal of Environmental Studies and Management, 6(5), 595–601. http://dx.doi.org/10.4314/ejesm.v6i5.3

Ajibade, I., McBean, G., & Bezner-Kerr, R. (2013). Urban flooding in Lagos, Nigeria: Patterns of vulnerability and resilience among women. Global Environmental Change, 23(6), 1714–1725. https://doi.org/10.1016/j.gloenvcha.2013.08.009

Alfa, M. I., Ajibike, M. A., & Daffi, R. E. (2018). Application of Analytic Hierarchy Process and Geographic Information System Techniques in Flood Risk Assessment: A Case of Ofu River Catchment in Application of analytic hierarchy process and geographic information system techniques in flood risk assessment. Journal of Degraded and Mining Lands Management, 5(4), 1363–1372. https://doi.org/10.15243/jdmlm.

Alimi, S. A., Oriola, E. O., Senbore, S. S., Alepa, V. C., Ologbonyo, F. J., Idris, F. S., Ibrahim, H. O., Olawale, L. O., Akinlabi, O. J., & Ogungbade, O. (2023). GIS-assisted flood-risk potential mapping of Ilorin and its environs, Kwara State, Nigeria. Remote Sensing in Earth Systems Sciences, 6, 239–253. https://doi.org/10.1007/s41976-023-00093-w

Al-Omari, A. A., Shatnawi, N. N., Shbeeb, N. I., Istrati, D., Lagaros, N. D., & Abdalla, K. M. (2024). Utilising remote sensing and GIS techniques for flood hazard mapping and risk assessment. Civil Engineering Journal, 10(5), 1423–1436. https://doi.org/10.28991/CEJ-2024-010-05-05

Arya, A. K., & Singh, A. P. (2021). Multi-criteria analysis for flood hazard mapping using GIS techniques: A case study of Ghaghara River basin in Uttar Pradesh, India. Arabian Journal of Geosciences, 14(8), 1–12.

Arya, D. S., & Singh, R. D. (2021). GIS-based flood hazard and vulnerability mapping: A case study from the Ganga River basin. Natural Hazards, 109(2), 2157–2178.

Behanzin, I. D., Thiel, M., Szarzynski, J., & Boko, M. (2016). GIS-based mapping of flood vulnerability and risk in the Bénin Niger River Valley. International Journal of Geomatics and Geosciences, 6, 1653–1669.

Birkmann, J. (2006). Measuring vulnerability to promote disaster-resilient societies: Conceptual frameworks and definitions. Natural Hazards, 38(1–2), 21–28. https://doi.org/10.1007/s11069-006-0024-7

Bui, D. T., Tsangaratos, P., Nguyen, V. L., et al. (2020). Comparative assessment of support vector machines and decision trees in flood susceptibility mapping at Hoa Binh province (Vietnam) using GIS and remote sensing techniques. Journal of Hydrology, 581, 124379.

Costache, R., & Bui, D. T. (2019). Flood susceptibility mapping using novel hybrid models based on the gravitational search algorithm and different machine learning classifiers. Journal of Hydrology, 575, 330–348.

Cutter, S. L., Boruff, B. J., & Shirley, W. L. (2003). Social vulnerability to environmental hazards. Social Science Quarterly, 84(2), 242–261. https://doi.org/10.1111/1540-6237.8402002

Danumah, J. H., Odai, S. N., Saley, B. M., Szarzynski, J., Thiel, M., Kwaku, A., … Akpa, L. Y. (2016). Flood risk assessment and mapping in Abidjan district using multi-criteria analysis (AHP) model and geoinformation techniques. Environmental Disasters, 3(1). https://doi.org/10.1186/s40677-016-0044-y

Desalegn, H., & Mulu, A. (2020). Flood vulnerability assessment using GIS at Fetam watershed, upper Abbay basin, Ethiopia. Heliyon. https://doi.org/10.1016/j.heliyon.2020.e05865

Elsheikh, R. F. A., Ouerghi, S., & Elhag, A. R. (2015). Flood risk map based on GIS and multi-criteria techniques (case study: Terengganu, Malaysia). Journal of Geographic Information System, 7, 348–357. https://doi.org/10.4236/jgis.2015.74027

Fatah, K. K., Mustafa, Y. T., & Hassan, I. O. (2022). Flood susceptibility mapping using an Analytic Hierarchy Process model based on remote sensing and GIS approaches in Akre District, Kurdistan Region, Iraq. Iraqi Geological Journal, 55(2C), 121–149. https://doi.org/10.46717/igj.55.2C.10ms-2022-08-23

Federal Emergency Management Agency (FEMA). (2020). Floods and floodplain management. https://www.fema.gov/nfip_sg_unit

Vanguard News. (2020, September). Buhari expresses shock over deaths, destruction of farms by flood in Kebbi. https://www.vanguardngr.com/2020/09/buhari-expresses-shock-over-deaths-destruction-of-farms-by-flood-in-kebbi/

Forkuo, E. K., & Adade, R. (2013). Flood hazard mapping using AHP and GIS: A case study of Accra, Ghana. Egyptian Journal of Remote Sensing and Space Science, 16(2), 251–261.

Forkuo, E. K., & Asare, Y. Mensa. (2012). River inundation and hazard mapping – A case study of the Susan River – Kumasi. In Proceedings of Global Geospatial Conference, Quebec City, Canada, May 14–17.

Ghosh, S., & Kar, S. K. (2018). A GIS and AHP-based flood hazard mapping approach for effective flood risk management. Modelling Earth Systems and Environment, 4(1), 27–38.

Gigovi´c, L., Pamu˘car, D., Baji´c, Z., Drobnjak, S., (2017): Application of GIS-Interval rough AHP methodology for flood hazard mapping in urban areas. Water 9 (360), 1–26.

Goepel, K. D. (2023). AHP Excel Template. https://bpmsg.com

Hu, S., Cheng, X., & Zhou, D. (2017). GIS-based flood risk assessment in suburban areas: A case study of the Fangshan District, Beijing. Natural Hazards,

87(3), 1525–1543. https://doi.org/10.1007/s11069-017-2828-0

Hussain, E., Ali, S., & Hafeez, M. M. (2021). Mapping flood hazard susceptibility using GIS and AHP: A case study of Jhelum River Basin. International Journal of Disaster Risk Reduction, 61. https://doi.org/10.1016/j.ijdrr.2021.102373

Hussain, M., Tayyab, M., Zhang, J., Shah, A. A., Ullah, K., Mehmood, U., & AlShaibah, B. (2021). GIS-based multi-criteria approach for flood vulnerability assessment and mapping in district Shangla: Khyber Pakhtunkhwa, Pakistan. Sustainability, 13, 3126. https://doi.org/10.3390/su13063126

Ifabiyi, I. P., & Ojoye, S. (2013). Rainfall trends in the Sudano-Sahelian ecological zone of Nigeria. Earth Science Research, 2(2), 194–202. https://doi.org/10.5539/esr.v2n2p194

Ikirri, M., Faik, F., Echogdali, F. Z., Antunes, I. M. H. R., Abioui, M., Abdelrahman, K., Fnais, M., Wanaim, A., Id-Belqas, M., & Boutaleb, S., (2022). Flood hazard index application in arid catchments: Case of the Taguenit Wadi watershed, Lakhssas, Morocco. Land, 11, 1178. https://doi.org/10.3390/land11081178

Intergovernmental Panel on Climate Change (IPCC). (2021). Climate change 2021: The physical science basis. Contribution of Working Group I to the Sixth Assessment Report of the Intergovernmental Panel on Climate Change. Cambridge University Press. https://doi.org/10.1017/9781009157896

Kebbi State Government. (2022). Kebbi State agricultural report 2022. Retrieved from https://www.kebbistate.gov.ng

Lyu, H.-M., Sun, W.-J., Shen, S.-L., & Arulrajah, A. (2018). Flood risk assessment in metro systems of mega-cities using a GIS-based modelling approach. Science of the Total Environment, 626, 1012–1025. https://doi.org/10.1016/j.scitotenv.2018.01.138

Mishra, K., & Sinha, R. (2020). Flood risk assessment in the Kosi megafan using multi-criteria decision analysis: A hydro-geomorphic approach. Geomorphology, 350, 106861. https://doi.org/10.1016/j.geomorph.2019.106861

Moll E. (2020): What Is a Semi-Arid Climate? sciencing.com; 2020. Accessed 04 September 2020.

Muis, S., Güneralp, B., Jongman, B., Aerts, J. C. J. H., & Ward, P. J. (2015). Flood risk and adaptation strategies under climate change and urban expansion. Nature Climate Change, 5, 1089–1093. https://doi.org/10.1038/nclimate2741

Muktar, A., & Yelwa, S. A. (2020). An analysis of the flood-prone areas in Birnin Kebbi using remote sensing and GIS. Journal of Geography, Environment and Earth Science International, 24(6), 77–85. https://doi.org/10.9734/jgeesi/2020/v24i630215.

Nigeria Emergency Management Agency (NEMA). (2022). Flood Disaster Report 2022. Daily Trust Newspaper, May 11.

Nigeria Hydrological Services Agency (NIHSA). (2019). 2019 Annual Flood Outlook for Nigeria.

Nigerian Hydrological Services Agency (NIHSA). (2023). Annual flood outlook report 2023. Abuja, Nigeria: NIHSA Press.

Ntajal, J., Lamptey, B. L., Mahamadou, I. B., & Nyarko, B. K. (2017). Flood disaster risk mapping in the Lower Mono River Basin in Togo, West Africa. International Journal of Disaster Risk Reduction, 23, 93–103. https://doi.org/10.1016/j.ijdrr.2017.03.015

Nyarko, B. K., Diekkrüger, B., Van De Giesen, N. C., & Vlek, P. L. G. (2015). Floodplain wetland mapping in the White Volta River Basin of Ghana. GIScience & Remote Sensing. https://doi.org/10.1080/15481603.2015.1026555

Ogato, G. S., Bantider, A., Abebe, K., & Geneletti, D. (2020). GIS-based multi-criteria analysis of flooding hazard and risk in Ambo Town and its watershed, West Shoa Zone, Oromia Regional State, Ethiopia. Journal of Hydrology: Regional Studies, 27, 100659. https://doi.org/10.1016/j.ejrh.2019.100659

Pham, B. T., Le, H. V., Prakash, I., et al. (2021). A comparative study of different machine learning models for flood susceptibility mapping in Vietnam. Environmental Earth Sciences, 80, 156.

Quesada-Román, A. (2022). Flood risk index development at the municipal level in Costa Rica: A methodological framework. Environmental Science & Policy, 133, 98–106.

Rahmati, O., Zeinivand, H., & Besharat, M. (2016). Flood hazard zoning using an ensemble modelling approach: a case study from Iran. Natural Hazards, 82(1), 453–479.

Rimba A.B, Setawati MD, Samba AB, Miura F. (2017): Physical flood vulnerability mapping applying geospatial techniques in Okazaki City, Aichi Prefecture, Japan. 2017;1(70): 1-22.

Rincón, D., Khan, U. T., & Armenakis, C. (2018). Flood risk mapping using GIS and multi-criteria analysis: A greater toronto area case study. Geosciences (Switzerland), 8(8), 275, https://doi.org/10.3390/geosciences8080275

Risi R. Jalayer F. De Paola, F. Lindley S. (2020): Delineation of flooding risk hotspots based on digital elevation model, calculated and historical flooding extents: the case of Ouagadougou. Stochastic Environmental Research and Risk Assessment. 2018; 32:1545–1559. Available: https://doi.org/10.1007/s00477-017-1450-8 Accessed 13 July 2020

Roosli, J. (2024). Risk assessment for the Kävlinge River for present and future climate scenarios using

HEC-RAS rain-on-grid (Master's thesis, Lund University). Lund University.

Saaty, T. L. (1980). The Analytic Hierarchy Process. McGraw-Hill.

Saaty, T. L. (2008). Decision making with the analytic hierarchy process. International Journal of Services Sciences, 1(1), 83–98.

Saber, M., Boulmaiz, T., Guermoui, M., Abdrabo, K. I., Kantoush, S. A., Sumi, T., … Mabrouk, E. (2023). Enhancing flood risk assessment through integration of ensemble learning approaches and physical-based hydrological modeling. Geomatics, Natural Hazards and Risk, 14(1). https://doi.org/10.1080/19475705.2023.2203798

Sadiq, I. U., Musa, A. A., & Shuaibu, M. (2022). GIS-based multi-criteria evaluation for flood hazard mapping in Nigeria: An application to Sokoto-Rima River Basin. Journal of Hydrology: Regional Studies, 39, 100971.

Sadiq, R., Akhtar, Z., Imran, M., & Ofi, F. (2022). Integrating remote sensing and social sensing for flood mapping. Remote Sensing Applications: Society and Environment, 25, 100697. https://doi.org/10.1016/j.rsase.2022.100697

Samela, C., Albano, R., & Sole, A. (2017). A GIS tool for cost-effective flood hazard mapping based on geomorphic methods: A case study in Southern Italy. Environmental Modelling & Software, 95, 90–107.

Samela, C., Albano, R., Sole, A., & Manfreda, S. (2018). A GIS tool for cost-effective delineation of flood-prone areas. Computers, Environment and Urban Systems, 70, 43–52.

Shale, G., Bantider, A., Abebe, K., & Geneletti, D. (2020). GIS-based multi-criteria analysis of flooding hazard and risk in Ambo Town and its watershed, West Shoa Zone, Oromia Regional State, Ethiopia. Journal of Hydrology: Regional Studies, 27, 100659. https://doi.org/10.1016/j.ejrh.2019.100659.

Sharma, S. V. S., Roy, P. S., Chakravarthi, V., & Rao, G. S. (2018). Flood risk assessment using multi-criteria analysis: A case study from Kopili River Basin, Assam, India. Geomatica, Natural Hazards and Risk, 9, 79–93.

Shuaibu, A., Hounkpè, J., Bossa, Y. A., & Kalin, R. M. (2022). Flood risk assessment and mapping in the Hadejia River Basin, Nigeria, using a hydro-geomorphic approach and multi-criterion decision-making method. Water, 14, 3709. https://doi.org/10.3390/w14223709

Subbarayan, S., & Sivaranjani, S. (2020). Modelling of flood susceptibility based on GIS and Analytic Hierarchy Process—A case study of the Adayar River Basin, Tamil Nadu, India. In I. Pal, J. von Meding, S. Shrestha, I. Ahmed, & T. Gajendran (Eds.), An interdisciplinary approach for disaster resilience and sustainability: Disaster Risk Reduction (Methods, Approaches and Practices) (pp. 91–110). Singapore: Springer. https://doi.org/10.1007/978-981-32-9527-8_6

Tehrany, M. S., Pradhan, B., & Jebur, M. N. (2015). Flood susceptibility mapping using a novel ensemble weight-of-evidence and support vector machine models in GIS. Journal of Hydrology, 512, 332–343.

Umar, A. T., Mashi, S. A., & Bako, M. M. (2020). Investigation of rainfall characteristics in the Sudano-Sahelian region of Nigeria (1971–2006). In Leal Filho, W. (Ed.), Handbook of Climate Change Resilience. Springer. https://doi.org/10.1007/978-3-319-93336-8_165

United Nations Development Programme (UNDP). (2006). Human Development Report 2006. http://hdr.undp.org/hdr2006/statistics/

United Nations Office for Disaster Risk Reduction (UNDRR). (2022). Global assessment report on disaster risk reduction 2022: Our world at risk – Transforming governance for a resilient future. United Nations. https://www.undrr.org/gar2022-our-world-risk

UNDP. (2010). Disaster risk reduction and climate change adaptation: Programming guidance note. United Nations Development Programme. https://www.undp.org/publications/disaster-risk-reduction-and-climate-change-adaptation-programming-guidance-note

Vojtek, M., & Vojteková, J. (2019). Flood susceptibility mapping on a national scale in Slovakia using the analytical hierarchy process. Water, 11(2), 364. https://doi.org/10.3390/w11020364

Wu Y, Zhong P, Zhang Y, Xu B, Ma B, Yan K. 2015. Integrated flood risk assessment and zonation method: a case study in Huaihe River basin. Nat Hazards. 78(1):635–651.

Yerima, B. D., & Bello, M. K. (2014). Assessment and planning for flood-prone areas in Birnin Kebbi, Kebbi State. International Journal of Environment, Ecology, Family and Urban Studies (IJEEFUS), 4(5).

Yonas, G. H., Andualem, T. G., Yibeltal, M., & Mengie, M. A. (2022). Flood hazard assessment and mapping using GIS integrated with multi-criteria decision analysis in Upper Awash River Basin, Ethiopia. Applied Water Science, 12, 148. https://doi.org/10.1007/s13201-022-01674-8

Youssef, A. M., & Hegab, M. A. (2019). Flood-hazard assessment modelling using multicriteria analysis and GIS: A case study—Ras Gharib area, Egypt. Elsevier.